Reprinted from

PHYSICA D

Physica D 92 (1996) 237–244

Mapping the channels of communication between the tropics and higher latitudes in the atmosphere

A.A. Tsonis[a,*], J.B. Elsner[b]

[a] *Department of Geosciences, University of Wisconsin-Milwaukee, Milwaukee, WI 53201-413, USA*
[b] *Department of Meterology, Florida State University, Tallahassee, FL 32306-3034, USA*

Received 12 June 1995; revised 4 September 1995; accepted 7 September 1995
Communicated by H. Flaschka

ELSEVIER

PHYSICA D

Nonlinear Phenomena

Aims and Scope

Physica D contains papers and review articles reporting experiments, techniques and ideas which, although they may be derived and explained in the context of a particular field, advance the understanding of nonlinear phenomena in general. Contributions of this type in the literature have dealt with: wave motion in physical, chemical and biological systems; chaotic motion in models relevant to turbulence; quantum and statistical mechanics governed by nonlinear field equations; instability, bifurcation, pattern formation and cooperative phenomena.

Abstracted/indexed in:
ACN Computing Reviews; Applied Mechanics Reviews; Current Contents: Physical, Chemical & Earth Sciences; EI Compendex Plus; Engineering Index; INSPEC; Physics Briefs

Subscription Information 1996
Physica A (ISSN 0378-4371). For 1996, Volumes 223–234 are scheduled for publication. Physica A is published semimonthly.
Physica B (ISSN 0921-4526). For 1996, Volumes 215–228 are scheduled for publication. Physica B is published semimonthly except in July, August, September, November and December.
Physica C (ISSN 0921-4534). For 1996, Volumes 256–279 are scheduled for publication. Physica C is published two to three times per month.
Physica D (ISSN 0167-2789). For 1996, Volumes 89–98 are scheduled for publication. Physica D is published semimonthly.
Subscription prices are available upon request from the Publisher. Combined subscriptions to Physica A, Physica B, Physica C and Physica D are available at a reduced rate. Subscriptions are accepted on a prepaid basis only and are entered on a calendar year basis. Issues are sent by SAL (Surface Air Lifted) wherever this service is available. Airmail rates are available upon request. Please address all your requests regarding orders and subscription queries to: *Elsevier Science B.V., Order Fulfilment Department, P.O. Box 211, 1000 AE Amsterdam, The Netherlands, Tel. + 31 20 4853642, Fax. + 31 20 4853598.* Claims for issues not received should be made within six months of our publication (mailing) date.

US mailing notice - Physica D (ISSN 0167-2789) is published semimonthly by Elsevier Science B.V., Molenwerf 1, P.O. Box 211, 1000 AE Amsterdam, The Netherlands. The annual subscription price in the USA is US$ 2836 (valid in North, Central and South America only), including air speed delivery. Second class postage paid at Jamaica, NY 11431.
USA POSTMASTERS: Send address changes to Physica D, Publications Expediting, Inc., 200 Meacham Avenue, Elmont, NY 11003. Airfreight and mailing in the USA by Publication Expediting.

℗ The paper used in this publication meets the requirements of ANSI/NISO 239.48-1992 (Permanence of Paper).

Printed in The Netherlands

ELSEVIER North-Holland, an imprint of Elsevier Science

ELSEVIER

Physica D 92 (1996) 237–244

PHYSICA D

Mapping the channels of communication between the tropics and higher latitudes in the atmosphere

A.A. Tsonis[a,*], J.B. Elsner[b]

[a]*Department of Geosciences, University of Wisconsin-Milwaukee, Milwaukee, WI 53201-413, USA*
[b]*Department of Meterology, Florida State University, Tallahassee, FL 32306-3034, USA*

Received 12 June 1995; revised 4 September 1995; accepted 7 September 1995
Communicated by H. Flaschka

Abstract

Nonlinear prediction is applied on atmospheric observations in order to derive seasonal to interannual predictability over the Northern Hemisphere. Using ideas from information theory we were then able from the spatial distribution of predictability to discover the exact location of corridors where "information" flows from the tropics to the midlatitudes. Here, information can be thought as a product or output of a physical entity such as El Niño or some other activity or phenomenon in the tropics whose fluctuations may often dictate large scale dynamics. The corridors are paths in the Pacific Ocean and the Atlantic Ocean and their exact location determines which areas on the globe are most likely to be affected from the interaction between the tropics and the midlatitudes.

PASC:
Keywords: Nonlinear prediction; Information flow; Climate dynamics; Predictability; Teleconnections; Annual cycle

1. Introduction

One of the paramount issues in atmospheric sciences is the equatorial to extratropical teleconnections and the interaction between the tropics and higher latitudes. Observational studies [4–7] have established the existence of teleconnections between regions in the tropics and regions in higher latitudes. These teleconnections are attributed to several atmospheric phenomena such as El Niño/Southern Oscillation (ENSO) (5), the 40–50 day oscillation [6,8], convective activity in the tropics [7] etc. Theoretical/modeling studies [9–12] have suggested and/or speculated on the mechanisms according to which teleconnections might be established. In general, it is proposed that they are established via equatorial Rossby waves (which travel westward) or Kelvin waves (which travel eastward) that are "allowed" to move northward to higher latitudes. It has also been suggested [13] that communication between tropics and midlatitudes may be happening through exporting of kinetic energy from low to higher latitudes. What, however, has not yet been established is the exact location and number of the corridors through which the communication between the tropics and midlatitudes is established. Here we

* Corresponding author.

SSDI 0167-2789(95)00265-0

applied ideas from chaos and information theories in order to obtain an answer to this problem. Our approach will also reveal the principal factors that determine the existence and location of these corridors.

2. Theory

From information theory [3] we know that for a continuous probability distribution the information content, I, is related to the Kolmogorov entropy, K, according to $\dot{I} = -K$ $(K > 0)$. For a time series the first derivative, $\dot{I}$, is equivalent to the mean loss of information per unit time. As it has been demonstrated in Wales [14], this loss of information is related to the *initial* decay of Pearson's correlation coefficient, $r(t)$, between forecast values of the time series and those actually observed according to

$$r(t) = 1 - C\,\mathrm{e}^{2Kt}, \tag{1}$$

where C and K are for stationary signals positive constants (see also Tsonis and Elsner [17]). The correlation coefficient ranges in magnitude between zero and one. We wish to stress that here $r(t)$ refers to the correlation coefficient that results from a prediction algorithm that explores the geometry of the state space (nonlinear prediction). Eq. (1) is independent of the prediction algorithm as long as it is a nonlinear approach but is not valid if $r(t)$ is obtained from statistical (linear) type forecast such as AR models, climatology, persistence etc. Such approaches may often display adequate predictive skills but have no connection to the mathematics that relate $r(t)$ to information loss. Between t_1 and t_2 the mean value of $r(t)$ will be given by

$$\bar{r} = 1/(t_2 - t_1) \int_{t_1}^{t_2} (1 - C\,\mathrm{e}^{2Kt})\,\mathrm{d}t$$

or considering that $\dot{I} = -K$

$$\bar{r} = 1 + \frac{C(\mathrm{e}^{-2\dot{I}t_2} - \mathrm{e}^{-2\dot{I}t_1})}{2\dot{I}(t_2 - t_1)}$$

or

$$\bar{r} = f(\dot{I}) \tag{2}$$

i.e. the mean loss of information over some time interval relates to the average predictability over this time interval via a function f. Let us assume now that we are dealing with a spatially extended system such as the atmosphere where a time series is available on every point of a latitude-longitude grid. If for a given longitude we take the derivative of Eq. (2) with respect to latitude (λ) we obtain

$$\frac{\mathrm{d}\bar{r}}{\mathrm{d}\lambda} = \frac{\mathrm{d}f(\dot{I})}{\mathrm{d}\lambda}$$

or

$$\frac{\mathrm{d}\bar{r}}{\mathrm{d}\lambda} = \frac{\mathrm{d}f(\dot{I})}{\mathrm{d}\dot{I}} \frac{\mathrm{d}\dot{I}}{\mathrm{d}\lambda}$$

or

$$\frac{\mathrm{d}\bar{r}}{\mathrm{d}\lambda} = A \frac{\mathrm{d}\dot{I}}{\mathrm{d}\lambda}. \tag{3}$$

Eq. (3) relates the north–south gradient of $\bar{r}$ to the north–south gradient of $\dot{I}$. Consequently, if a spatial distribution of $\bar{r}$ is provided, then the potential exists to identify regions on Earth where the rate of loss of information per distance is slow thereby mapping the channels along which information flows easily. Note that according to information theory an information source is a mathematical model for a physical entity that produces a succession of symbols called outputs. There are many different symbols that can be produced by a source and the space that contains all those symbols is called the alphabet of the source. In our problem the alphabet may contain many different "symbols" that can be exchanged. The symbols can be fluctuations due to El Niño or any other kind of fluctuations such as convective activity in the tropics, the 40–50 day oscillation, etc., that can be exchanged between the tropics and midlatitudes through any type of interaction.

3. Data analysis and results

We now proceed to obtain a map of the spatial distribution of $\bar{r}$. The data used consist of monthly 500 hPa geopotential height time series in 1,080 grid points in the Northern Hemisphere. Geopotential heights at a fixed pressure level indicate the density in the underlying atmosphere. The points are arranged on a grid between 20° N and the North Pole having a latitude-longitude resolution of 4×6 degrees. Each time series spans the period from January 1946 to June 1989 (522 values). Due to the need for a sufficient sample size in the following calculation we were forced to restrict our calculations in the above mentioned part of Northern Hemisphere only. In order to estimate the value of $\bar{r}$ for each grid point we applied nonlinear prediction on each and every one of the 1,080 univariate time series. The nonlinear prediction model was a version of the Farmer and Sidorowich [1] and Sugihara and May [2] interpolative algorithm used in Wales [14] which is based on the simplex method in phase space. For each grid point an embedding dimension (n) is chosen and a phase space having as coordinates the corresponding time series $x(t_i)$ and its successive time shifts (delays) is constructed. This vector time series given by

$$X(t_i) = \{x(t_i),\ x(t_i + \tau) \ldots x(t_i + (n-1)\tau)\}\ ,$$

where τ is an appropriate delay. Based on the decay of the autocorrelation function [15] a time delay of two months is used, however, results were not sensitive to the exact choice of a time delay in the range of one to twelve months. For each grid point a "window" containing the first 480 values of $x(t_i)$ is adapted and the corresponding points in phase space are produced. Then the terminal point is located and a minimal neighborhood is defined around it such that the sequence containing the terminal point is located within the simplex with the minimum diameter formed from the $n+1$ closest neighbors. A one month prediction is then made by deriving the mapping that dictates the motion of the points in the neighborhood after one month into their future. Then the predicted point becomes the terminal point and the procedure is repeated in order to obtain a two month forecast and so on up to twelve months. Subsequently, we shift the window by one value (so now values 2 to 481 are considered) and the above sequence of operations is repeated thus obtaining another 12-month prediction and so on until we run out of data. Finally, from all twelve-month predictions we calculate the correlation coefficient between the predicted and actual values, $r(t)$, for $t = 1, 12$. Accordingly, $r(t)$ values are based on sample sizes of about forty. A measure of predictability is then obtained for each grid point by computing the average correlation coefficient

$$\bar{r} = \tfrac{1}{12} \sum_{t=1}^{12} r(t)\ .$$

The choice of a year as our averaging time, even though is rather arbitrary, represents how well the time series can be predicted on average over a period which is commensurate with the standard cycle of a major external forcing. The predictability field is then contoured on a map of the Northern Hemisphere (20° N–90° N) (Fig. 1). In all the above calculations we used an embedding dimension of five. This was decided after applying the procedure of Sugihara and May [2] who suggest plotting the one step (one month) prediction error as a function of the embedding dimension. For all grid points we noticed that $r(1)$ increased from low embedding dimensions and saturated above embedding dimension four. Sensitivity tests using embedding dimensions in the range of four to eight indicates that the results remain unaffected. We wish to stress at this point that we have kept the annual cycle in our analysis. As it is explained in Fig. 2 the character of the annual cycle is, dynamically speaking, not unique. The annual cycle can be a periodic function or a quasi-periodic function or a chaotic function depending on the location. Thus, since the annual cycle represents the major forcing in our climate system, when we explore geometry in state space or nonlinear

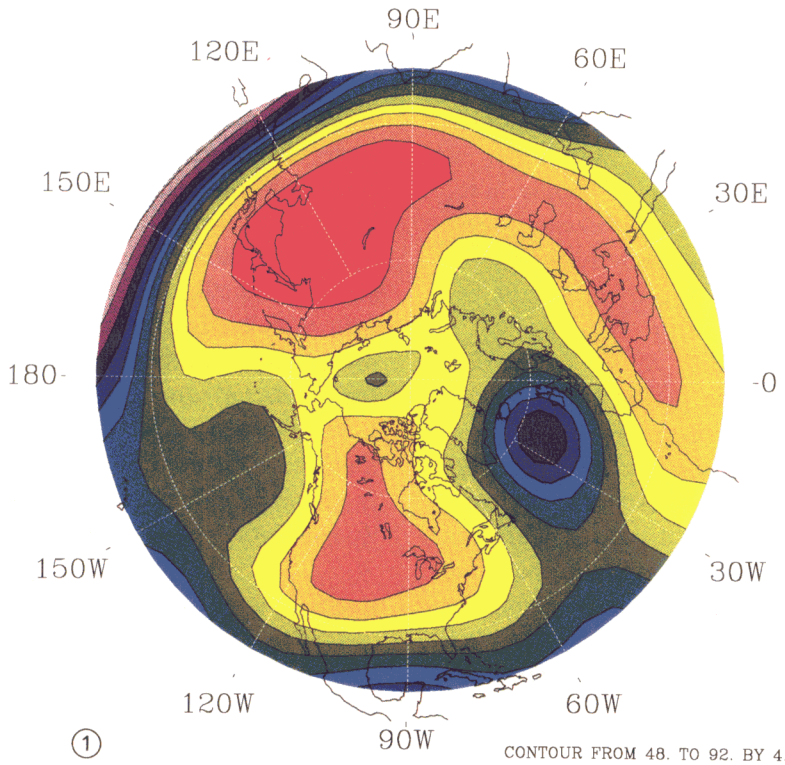
90E
120E
60E
150E
30E
180
0
150W
30W
120W
60W
90W
1
CONTOUR FROM 48. TO 92. BY 4.

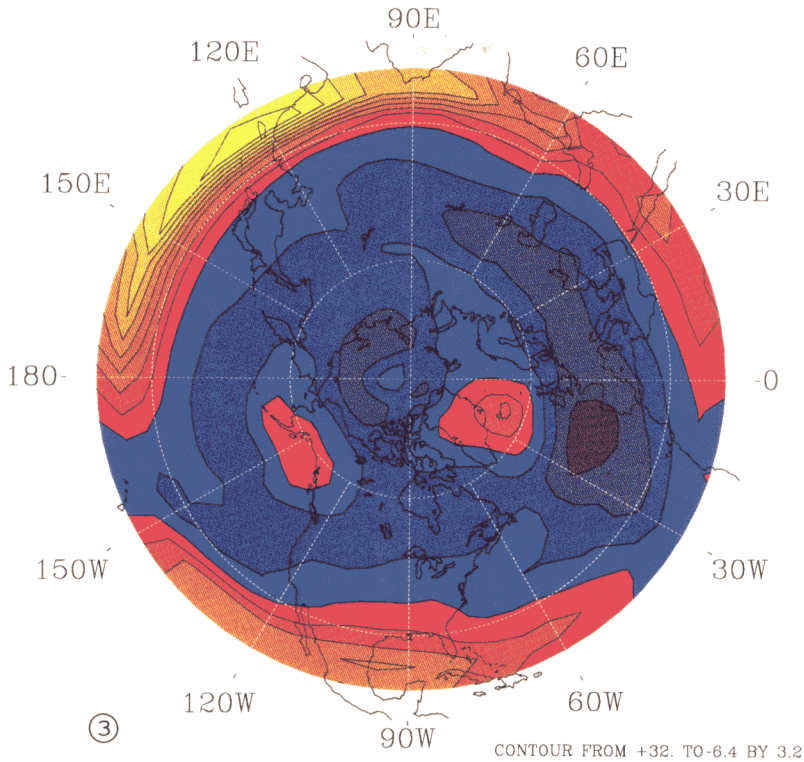
90E
120E
60E
150E
30E
180
0
150W
30W
120W
60W
90W
3
CONTOUR FROM +32. TO-6.4 BY 3.2

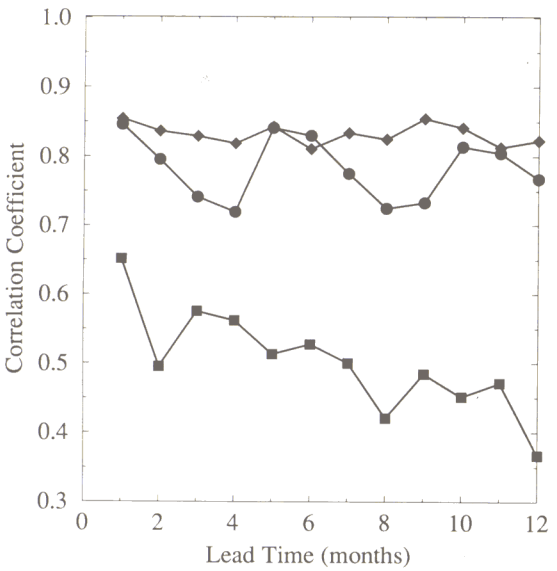

Fig. 2. Nonlinear prediction can provide information about the underlying a time series dynamics. A "flat" $r(t)$ indicates that the correlation coefficient between actual and predicted values is independent of the forecast time and corresponds to periodic signals. An oscillating about a constant level $r(t)$ is indicative of quasi-periodic signals. A decaying with time $r(t)$ indicates chaotic behavior. The above characteristics apply when additive noise is present. Additive noise produces a constant offset in the correlation but it would not obliterate the general behavior of periodic, quasi-periodic or chaotic signals. Here we show $r(t)$ vs. t for three different locations in Northern Hemisphere. Diamonds correspond to the point with coordinates 46° N, 186° E (midlatitudes), circles to the point with coordinates 90° N, 0° E (N. Pole) and squares to the point with coordinates 20° N, 270° E (subtropics). Apparently those three locations exhibit different dynamics as one corresponds to a periodic signal one to a quasi-periodic signal and one to a chaotic (nonperiodic) signal. Thus the annual cycle cannot be assumed as exhibiting a unique dynamic behavior on all locations on Earth.

dynamics in our data we cannot and should not simply remove it by subtracting the climatological mean monthly values as we do when we statistically study anomalies. Keeping the annual cycle is consistent with previous findings that have tied the annual cycle to ENSO dynamics [16] and with very recent results which show that over the last 300 years the annual cycle has not remained constant in time [17]. We will return to this issue later.

Returning to Fig. 1, we observe areas of high predictability (over China and the United States) and areas of low predictability (over northern Atlantic Ocean and western Pacific Ocean in the subtropics). Note that due to time scales involved in our sampling and in our analysis, Fig. 1 displays to a large extent the effect of the annual cycle. The latitudinal distribution of the annual cycle depends largely on the distribution of land and water and on the available insolation at each latitude. The annual cycle is most pronounced over midlatitude continental regions and less over the oceans and at lower latitudes. The high predictability of the seasonal cycle over continental regions can be explained by the strong dependence of lower tropospheric temperatures (and thus density) to changes in solar insolation which cause drastic changes in atmospheric circulation patterns. For example, during the summer Asia is warmed and as a result the Siberian anticyclone decays and is replaced by the South Asia cyclone. This dependence is much weaker over large ocean regions where sensible heat

Fig. 1. Spatial distribution of predictability as measured by the quantity $\bar{r}$ ($\times 100$) (an average correlation between actual and predicted 500 hPa geopotential height values) defined in the text. Correlations range from about 0.5 (violet) to about 0.9 (red). Results have been smoothed using a nine-point uniform filter. Spatial heterogeneity of seasonal to interannual predictability is clearly evident.

Fig. 3. The north–south gradient of Fig. 1. According to Eq. (4) this map shows regions where the loss of information per distance is fast (i.e. information is not transported easily) [yellow–red] and regions where the loss of information per distance is slow or slightly negative (i.e. information from lower latitudes is transported easier to midlatitudes) [light blue to purple]. Two corridors along which information is transported easily, one over the Pacific Ocean and one over the Atlantic Ocean have been discovered.

from water can significantly modulate temperatures in the lower troposphere and in the tropics where solar insolation is fairly constant. The expected low predictability over oceanic regions seems to have been accentuated in northern Atlantic Ocean where the predictability is much poorer compared to similar regions over northern Pacific Ocean that normally receive equal amounts of solar insolation. This feature may be attributable to the Gulf Stream and/or to the North Atlantic deep water [18]. Both these "signals" give off great amounts of heat in the North Atlantic Ocean thereby making winters over those areas milder. This reduces the amplitude of the seasonal cycle whose predictability drops. Similar comments can be made about the predictability over the subtropical western Pacific Ocean where the values are much lower than those over the subtropical eastern Pacific. This feature is attributable to the seasonal to interannual footprint of the chaotic (and thus unpredictable) ENSO signal [19–21]. Overall the nonlinear prediction results despite limited data amounts reproduce accurately the global climatological picture and thus provide confidence about our procedure. This is extremely important because it is only through nonlinear prediction and Fig. 1 that one can proceed to map the channels of communication between tropics and higher latitudes.

For the dynamical system in question and time scales involved (i.e. $t_2 = 12$ months, $t_1 = 1$ month) it follows that in Eq. (3)

$$A = [(-24\dot{I} - 1)\,\mathrm{e}^{-24\dot{I}} + (2\dot{I} + 1)\,\mathrm{e}^{-2\dot{I}}]\frac{C}{22\dot{I}^2}$$

which is positive for all $K > 0$ or all $\dot{I} < 0$. We thus can write

$$\frac{\mathrm{d}\bar{r}}{\mathrm{d}\lambda} \propto \frac{\mathrm{d}\dot{I}}{\mathrm{d}\lambda}. \tag{4}$$

Since the geographical distribution of r and $\bar{r}$ depends strongly on the distribution of land and water and on the two large climate signals mentioned above (which are not necessarily functions of λ), we can consider that r and $\bar{r}$ do not depend strongly on λ. Then Eq. (4) dictates that the north–south gradient of $\bar{r}$ is proportional to the north–south gradient of the rate of loss of information, and its interpretation is straight forward. If the gradient of $\bar{r}$ is significantly greater than zero then the rate of loss of information per distance is fast (thus information is not transported easily from lower to higher latitudes). If the gradient approaches zero or becomes negative then the rate of loss of information per distance slows or becomes negative (i.e. information is transported easier). By applying the above ideas to Fig. 1, we can derive a map that shows where information flows easier thus defining corridors of communication between the tropics and higher latitudes. Fig. 3 shows the north–south gradient of $\bar{r}$. Yellow corresponds to $\mathrm{d}\bar{r}/\mathrm{d}\lambda = 0.34$ which given the range of $\bar{r}$ in Fig. 1, represent a value significantly greater than zero. As we go from yellow to red $\mathrm{d}\bar{r}/\mathrm{d}\lambda$ decreases approaching zero for light blue and becoming slightly negative for darker blue and purple. From the above discussion and arguments two corridors along which information flows easily (channels of communication) can be identified. One in the Pacific Ocean (centered around 160° W) and a wider one in the Atlantic Ocean (centered around 25° W).

The delineation of these channels of communication provides new insights to our knowledge about large scale dynamics in the atmosphere. First, their existence verifies model results that have suggested or speculated the existence of such regions [8,11] but not the exact location and number. The existence of the corridors may explain teleconnections since their location determines where information leaks into higher latitudes. For example, according to Fig. 3, El Niño related fluctuations trigger Rossby waves that emanate to higher latitudes at about 160° W longitude. The subsequent interaction between those fluctuations (or the triggered waves) and the general circulation will result in changes of a certain horizontal scale. Since the immediate

land areas are those of the United States and Canada those areas are most likely to be affected. We can thus establish teleconnections between El Niño and changes to weather patterns in North America. Our results may also explain the observed by the general circulation models phase-locked response [11] at higher latitudes in the northern Pacific Ocean and America. This phase-locking refers to similar responses irrespective of the place of origin and the nature of the fluctuations in the tropics. We suggest that because the corridor is rather narrow, the fluctuations trigger waves that emanate into higher latitudes more or less from the same region. Thus they transport information at the same location regardless of the source. A similar to Eq. (4) may be derived for the longitudinal (east–west) gradient of $\bar{r}$. This gradient, however, is very weak (varying from -0.015 to 0.015) indicating the direct and easy communication due to the prevailing zonal circulation. This result indicates that the information flow has a much greater (more than an order of magnitude) meridional component than a zonal component and thus it is mostly restricted to the meridional direction. Whether or not similar corridors exist in the South Hemisphere remains to be seen until more data become available there. Hopefully, our results together with theories of atmospheric teleconnections will enhance our understanding of the interactions taking place on our planet and of their effects on weather and climate.

4. Concluding remarks

It is interesting to speculate about the physical connection of predictability to dynamics and about the underlying physics *over the time scales involved in our study*. Our results depend on retaining the annual cycle in our data. If the annual cycle is removed the resulted Fig. 1 makes no sense whatsoever as it loses all its structure and climatology and simply shows noise. Since the annual cycle is more pronounced (and thus more predictable) in the midlatitudes than in the tropics, according to Eq. (4) information has to flow from tropics to higher latitudes. This "direction" seems to be solely due to the annual cycle. Thus, firstly our results suggest a greater role for the annual cycle in large scale dynamics that it is traditionally practiced. Secondly, since the delineation of Figs. 1 and 3 is a direct result of how the spatial distribution of the predictability of the annual cycle signal is modified by basically the El Niño and the North Atlantic signals, our results may be suggesting that, to a large degree, global scale dynamics arise from the interplay of three major signals: annual cycle, El Niño, and the North Atlantic signal.

Our approach provides a unique example of how a combination of ideas from the theories of chaos and information applied to a geophysical field can yield significant and novel insight concerning the physics of our climate system. At the same time because of its general character our approach could be applied to other spatially extended systems with infinite degrees of freedom such as in fluid dynamical systems, chemical and biological systems, etc. [15].

Acknowledgements

Parts of this work were supported by NSF grants ATM-9310959 and ATM-9310715.

References

[1] J.D. Farmer and J.J. Sidorowich, Phys. Rev. Lett. 59 (1987) 845.
[2] G. Sugihara and M. May, Nature 344 (1990) 734.
[3] C. Shannon and W. Weaver, The Mathematical Theory of Communication (Illinois Univ. Press, Urbana, 1949).
[4] J.M. Wallace and D.S. Gutzler, Mon. Wea. Rev. 109 (1981) 784.
[5] J.D. Horel and J.M. Wallace, Mon. Wea. Rev. 109 (1981) 813.

[6] K.-M. Lau and P.H. Chan, Mon. Wea. Rev. 113 (1985) 1889.
[7] T.N. Parmer and J.A. Owen, Mon. Wea. Rev. 114 (1986) 648.
[8] R. Madden and P.R. Julian, J. Atmos. Sci. 28 (1971) 702.
[9] B.J. Hoskins and D.J. Karoly, J. Atmos. Sci. 38 (1981) 1179.
[10] K.-M. Lau and L. Peng, J. Atmos. Sci. 44 (1987) 950.
[11] P.J. Webster, J. Atmos. Sci. 39 (1982) 41.
[12] P.J. Webster and H.-R. Chang, J. Atmos. Sci. 45 (1988) 803.
[13] A. Wiin-Nielsen and T.-C. Chen, Fundamentals of Atmospheric Energetics (Oxford, New York, 1993).
[14] Wales, D.J. Nature 350 (1991) 485.
[15] A.A. Tsonis, Chaos: From Theory to Applications (Plenum, New York, 1992).
[16] E.M. Rasmusson, X. Wang and C.F. Ropelewski, J. Marine Syst. 1 (1990) 71.
[17] D.J. Thomson, Science 268 (1995) 59.
[18] W.S. Broecker and G.H. Denton, Sci. Amer. 262 (1990) 49.
[19] G.K. Vallis, Science 232 (1986) 243.
[20] A.A. Tsonis and J.B. Elsner, Nature 358 (1992) 217.
[21] J.B. Elsner and A.A. Tsonis, Geophys. Res. Lett. 20 (1993) 213.